Biomimetic Growth of Hydroxyapatite on Kenaf Fibers

Saiful Izwan Abd Razak,[a,b,*] Izzati Fatimah Wahab,[b] Mohammed Rafiq Abdul Kadir,[b] Ahmad Zahran Md Khudzari,[a,b] Abdul Halim Mohd Yusof,[c] Farah Nuruljannah Dahli,[c] Nadirul Hasraf Mat Nayan,[d] and T. Joseph Sahaya Anand [e]

Biomimetic hydroxyapatite (HA) growth on mercerized kenaf fiber (KF) was achieved by immersion in a simulated body fluid (SBF) solution with the addition of a chelating agent. An electron micrograph revealed uniform HA layers on the KF within 14 days of immersion with significant vibrational peaks of HA components. The tensile tests showed no significant drops in the unit break of the modified fibers. This new bone-like apatite coating on KF can be useful in the field of bone tissue engineering. The key motivation for this new approach was that it utilizes the abundantly available kenaf plant resource as the biobased template.

Keywords: Kenaf fiber; Simulated body fluid; Hydroxyapatite; Bone repair materials

Contact information: a: IJN-UTM Cardiovascular Engineering Centre, Universiti Teknologi Malaysia, 81310 Skudai, Johor, Malaysia; b: Faculty of Biosciences and Medical Engineering, Universiti Teknologi Malaysia, 81310 Skudai, Johor, Malaysia; c: Faculty of Chemical and Energy Engineering, Universiti Teknologi Malaysia, 81310 Skudai, Johor, Malaysia; d: Faculty of Engineering Technology, Universiti Tun Hussein Onn Malaysia, 86400 Batu Pahat, Johor, Malaysia; e: Faculty of Manufacturing Engineering, Universiti Teknikal Malaysia Melaka, 76100, Durian Tunggal, Melaka, Malaysia;
**Corresponding author: saifulizwan@utm.my*

INTRODUCTION

Bone tissue engineering aims to induce new functional bone regeneration *via* the synergistic combination of biomaterials, cells, and factor therapy with the ultimate goal of creating bone grafts that enhance bone repair and regeneration (Amini *et al.* 2012). Natural bone is a composite material composed of a collagen matrix reinforced with hydroxyapatite (HA) crystals. Forming an HA coating *via* a biomimetic route (immersion in simulated body fluid (SBF)) can be considered a moderate way to grow an apatite layer on a substrate (Sukhorukova *et al.* 2015). Bioactivity of artificial bone material *in-vitro* can be evaluated through utilization of this method because its composition is very close to that of human blood plasma. The HA grown using this method is similar to the human bone mineral, which is why it is often called bone-like apatite (An *et al.* 2015). The most commonly explored porous bone scaffold materials include bioceramics and bioactive glass (Chen *et al.* 2013; Chen *et al.* 2014) and polymers (Owen *et al.* 2016). Plus there are many kinds of biocompatible materials have been used to guide mineralization of HA to make them suitable as bone repair materials, including ceramics (Dai *et al.* 2015), metallics (Wang *et al.* 2015), polymeric materials (Huang *et al.* 2015), and their composites (Guo *et al.* 2015), cellulose (Li *et al.* 2012; Morimune-Moriya *et al.* 2015), and collagen (Tomoaia and Pasca 2015).

Kenaf (*Hibiscus cannabinus* L., Malvaceae) is a warm, seasonal, annual, fiber crop. It is a fiber plant native to east central Africa, where it has been grown for several thousand years for food and fiber. In Malaysia, kenaf is treated as a renewable commodity that can

be transformed into a new source of growth to diversify the country's commodities sector. The Malaysian government established the National Kenaf and Tobacco Board in 2009 to implement policies and developmental agendas to ensure the viability of the kenaf industry (Juliana *et al.* 2012). The chemical content of kenaf fiber is given in Table 1 (Wambua *et al.* 2003). Various applications have been explored to utilize kenaf fiber (KF), including using it as an adsorbent material (Zaini and Kamarudin 2014), for feedstock (Saba *et al.* 2015), insulation board (Fernando *et al.* 2015), and paper (Gao *et al.* 2015); and as reinforcement in polymer composites (Razak *et al.* 2013). In light of the fact that kenaf is abundant and useful, it is interesting to explore the potential use of kenaf as a bone repair material.

Table 1. Chemical composition of KF

Chemical composition	%
Cellulose	69
Lignin	3
Hemicellulose	27
Ash	1

Lignocellulose- and cellulose-based materials have no ability to form HA or can be regarded as non-bioactive because their surface functional groups primarily consist of OH. The absence of net charge is not favourable for any HA growth. Therefore, the use of a chelating agent that can bind the metal ions during the SBF immersion is vital (Zollfrank *et al.* 2012). Citric acid is a strong chelating agent for bonding calcium ions to its carboxylic groups; it promotes HA nucleation in a 1.5 SBF solution (Rhee and Tanaka 2000; Sánchez-Ferrero *et al.* 2015) and exists in its citrate form in fresh bone (Costello *et al.* 2014).

The reasoning behind lignocellulosic fibers such as KF being selected for use as supporting scaffolds is their abundance and renewability (Gan *et al.* 2015), good mechanical properties (Fiore *et al.* 2015), biodegradability (Won *et al.* 2014), negligible to foreign body, and inflammatory response reactions (Kulma *et al.* 2015). Furthermore there are reports showing enhanced osteoblast cell attachment on mineralized electrospun pure cellulose surface (Rodríguez *et al.* 2011, 2014).

To date, there are limited studies focusing on the biomimetic growth of HA on natural fibers using SBF and, in particular, KF. Therefore, the main goal was to grow HA on KF using SBF with the addition of citric acid. It is expected that the KF could be modified to be bioactive using a chelating agent, which would promote growth of HA crystals during the SBF immersion. Prior to SBF immersion, the KF was treated using a conventional mercerization process.

EXPERIMENTAL

Mercerization of KF

Raw untreated kenaf bast fibers (KF) (Everise Crimson (M) Sdn. Bhd., Malaysia) were mercerized using a 6 wt.% NaOH solution. This NaOH concentration was chosen based on optimum mercerization concentration of KF toward its unit break properties (Edeerozey *et al.* 2007). The small bundle of KF was cut approximately 60 mm in length

and soaked in the NaOH solution for 3 h at 95 °C. Then, the mercerized KF were rinsed thoroughly to obtain a pH of 7 and later dried for 24 h at 90 °C.

Preparation of SBF Solution

Table 2 compares the ion concentration of human blood plasma, SBF, and 1.5 SBF. A 1.5 SBF solution (1.5 times higher ion concentration than the SBF) was prepared by dissolving reagent-grade NaCl, $NaHCO_3$, KCl, $K_2HPO_4 \cdot 3H_2O$, $MgCl_2 \cdot 6H_2O$, $CaCl_2$, and Na_2SO_4 in ion exchanged distilled water according to Table 1.

The solution was buffered at a pH of 7.4 with tris(hydroxymethyl) aminomethane at 37% (HCl) at 36.5 °C. Citric acid (Sigma) was dissolved into the 1.5 SBF solution to provide a concentration of 1mM, and the pH was readjusted with tris(hydroxymethyl) aminomethane to 7.4 (Rhee and Tanaka 2000; Kokubo and Takadama 2006; Li *et al.* 2012).

Table 2. Ion Concentration of Human Blood Plasma, SBF, and 1.5×SBF Solutions (mM)

Component	Na^+	K^+	Ca^{2+}	Mg^{2+}	Cl^-	HPO_4^{2-}	HCO_3^-	SO_4^{2-}
Blood plasma	142	5.0	2.5	1.5	103	1.0	27	0.5
SBF	142	5.0	2.5	1.0	126	1.0	10	1.0
1.5 SBF	213	7.5	3.75	1.0	189	1.5	15	1.5

Growth of HA

Kenaf fibers (2 g) were immersed in 30 mL of prepared 1.5 SBF solution with and without the addition of citric acid. The containers were placed in a covered water bath at a controlled temperature of 37 °C. The immersed KF were then collected at intervals of 7 and 14 d to evaluate the HA growth and later dried for 24 h at room temperature.

Characterization

Scanning electron microscope (SEM) images were obtained using a Leo Supra (50VP, Carl Zeiss, Germany) equipped with an energy dispersive X-ray (EDX) system. Samples were sputter-coated with platinum before SEM observation. Coating thickness of HA was reported using the difference between average radius of the uncoated KF and average radius of the KF/HA observed under SEM.

Fourier transform infrared (FTIR) spectra of the samples were obtained using a Perkin Elmer Spectrum System (2000 FTIR, USA) with a resolution of 4 cm^{-1} averaging 16 scans. Pulverized samples were diluted with KBr powder by one tenth, and the background was normalized with neat KBr data.

The fiber-bundle tensile tests were performed using a computer controlled Instron machine (USA) with a crosshead speed of 1 mm/min at a standard laboratory atmosphere of 23 °C. Samples were cut into 60 mm lengths and separated into individual fiber bundles. The gauge length was approximately 25 mm. Twenty replications were done for each fiber type. Diameters of the fibers were taken as an average of three readings along the length of the fibers. The gripping technique was in accordance with ASTM D3822 (2007). Fibers were conditioned in an environment with an ambient temperature of 23 °C and a relative humidity of 30 to 40% for over 24 h prior to tests. The moisture content of the fibers were approximately 8.5% during the tensile tests.

RESULTS AND DISCUSSION

Morphological Analysis and EDX

Figure 1a depicts the SEM image of the untreated KF. The image clearly shows typical surface features of untreated lignocellulosic fibers and the presence of impurities on the surface of the fiber. Moreover, the majority of the fiber is covered by hemicelluloses and lignin. Figure 1b reveals the image of the obtained untreated KF after soaking in 1.5 SBF solution at 36.5 °C for seven days. Traces of segregated spherulite were observed on the fibers. The surface of the native fiber is exposed, with no major crystal deposition. Untreated lignocellulosic fibers, like KF, contain lignin, which is rich in carboxylic groups. The carboxylic groups of lignin could form electrostatic interactions between the fibers and the calcium ions in the solution and then induce the heterogeneous nucleation of HA (Morimune-Moriya *et al.* 2015). Because lignin is not a major constituent in KF (3% of KF (Akil *et al.* 2011)), the chance for HA nucleation is low. Furthermore, the OH groups of cellulose are considered to be bio-inert in terms of apatite forming ability because of the absence of a net charge. It can be seen in Fig. 1c that the mercerized fiber surface is clean, with no significant impurities. Furthermore, the surface topography reveals the emergence of the fiber bundle morphology with more exposed OH groups. This is attributable to the partial removal of surface hemicelluloses and lignin by the mercerization treatment. After soaking in 1.5 SBF without any citric acid (Fig. 1d) for seven days, no HA crystals were observed on the mercerized fiber. This indicates that the KF is dominated by the bio-inert OH groups. With the presence of citric acid during the seven days of SBF soaking (Fig. 1e), a large number of HA crystals can be identified on the mercerized fiber. The microstructures were quite similar to those of HA on bioactive glass (Sola 2011). The mercerized fiber opened up more OH groups to become exposed to the citric acid for chelation with Ca ions. A higher magnification (Fig. 1f) reveals that the HA coating consisted of porous spheroidal formations, which can alternatively be viewed as single crystalline nano-platelets forming spheroid aggregates. Fourteen days of SBF soaking (Figs. 2g and 2h) with citric acid, however, induced more uniform HA crystal layers on the KF. The HA cannot move freely, as they are bound to the fiber, which acts as a supporting scaffold for the HA. It is clear that the surface groups of the KF relates to the growth of the HA compound. Seven days of soaking in SBF with the addition of citric acid yielded porous spheroids. Once the initial layer has been formed, further growth of HA surrounds the KF. The Ca/P ratio of the sample (Table 2) revealed that the apatite had a higher percentage of calcium after seven days of incubation and a higher amount of phosphate after fourteen days of incubation.

Table 2. Particle Size, Coating Thickness, and Ca/P Ratio of KF Determined by EDX

Sample	Particle size (μm)	Coating thickness (μm)	Ca/P ratio
Untreated KF-SBF	1-2	Scattered	N/A
Mercerized KF-SBF without citric acid	N/A	N/A	N/A
Mercerized KF-SBF with citric acid for 7 d	1-2	3-4	2.3
Mercerized KF-SBF with citric acid for 14 d	Layered	5-6	1.72

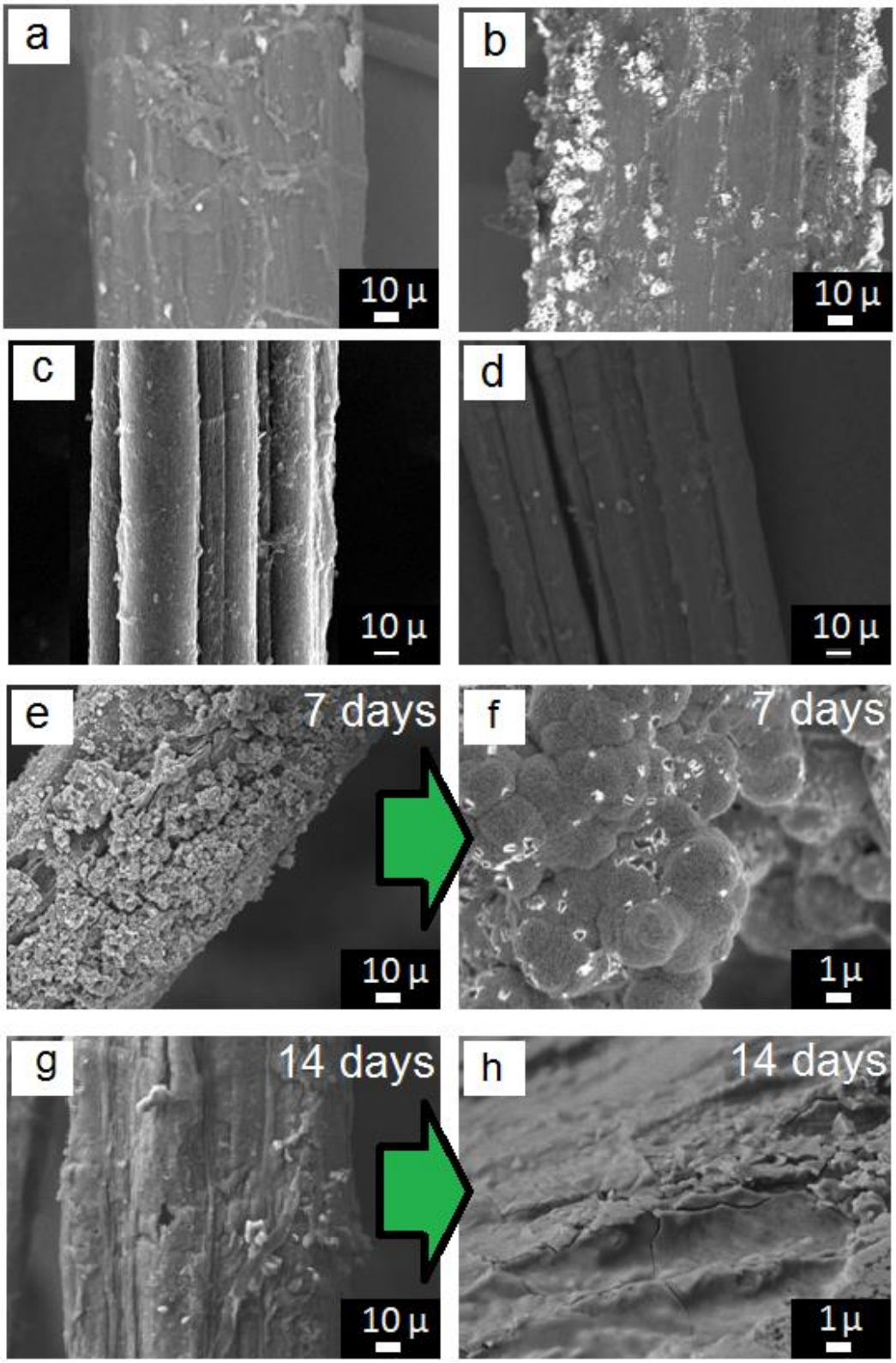

Fig. 1. SEM images of a) untreated KF, b) untreated KF/HA, c) mercerized KF, d) mercerized KF/HA without citric acid, e-f) mercerized KF/HA with citric acid (7 d), and g-h) mercerized KF/HA with citric acid (14 d).

FTIR Spectroscopy

The FTIR spectrum of the control (KF) in Fig. 2a exhibited a band at 3400 cm^{-1}, which represents the intermolecular and intramolecular H bonds of free OH in cellulose. Figure 2a also displays a C-H stretching peak at 2900 cm^{-1}, as well as a peak at 1700 cm^{-1}, which represents the C=O stretching (acetyl group of hemicellulose and ester linkage of lignin). These IR vibrations are in agreement with the functional groups of lignocellulosic fiber. It can be seen in Fig. 2b that mercerization resulted in an increased detection of the OH band compared to the untreated KF, mostly because more cellulose surfaces were exposed due to NaOH treatment (Edeerozey *et al.* 2007).

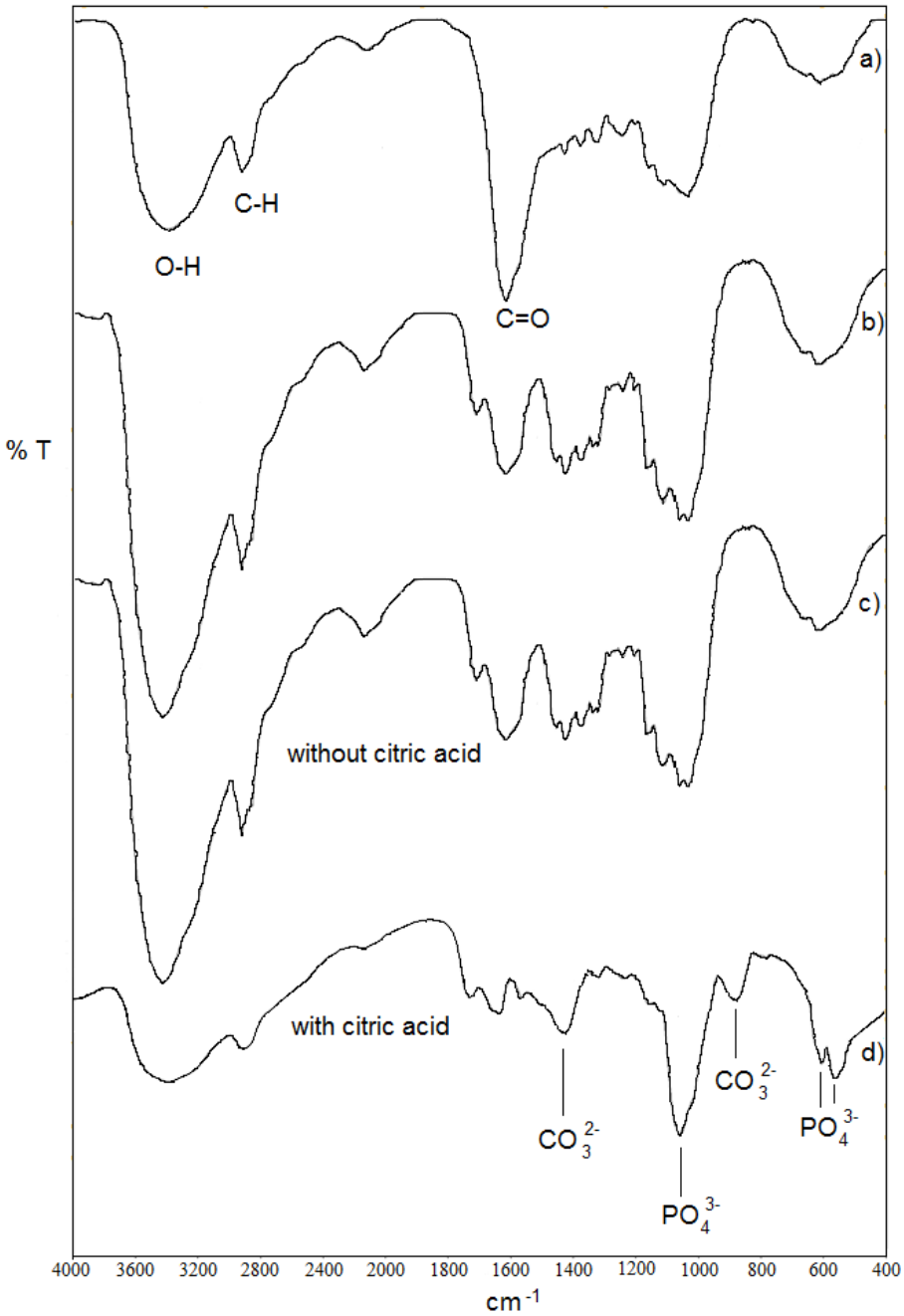

Fig. 2. FTIR spectra of a) untreated KF b) mercerized KF c) mercerized KF/HA-14 days (without citric acid) d) mercerized KF/HA-14 days (with citric acid).

Without the addition of citric acid (Fig. 2c), the KF showed no vibrational peaks resembling those of HA, even after immersion in SBF for fourteen days. This was because there are no energetically preferential sites for the calcium to bind onto to form and grow HA nuclei. The sample of mercerized KF with the addition of citric acid during the SBF immersion (Fig. 2d) revealed several new peaks related to the HA formation. The stretching modes of phosphate ions were observed at 1050, 605, and 570 cm^{-1}. Meanwhile, peaks at 1423 and 880 cm^{-1} represent the out-of-plane stretching mode of carbonate ions (Pylypchuk *et al.* 2015). It can be said that the HA crystals that formed on the mercerized KF were carbonate-containing HA. Reduction of the 3400 and 1700 cm^{-1} peaks signify the surface of the KF being covered with the HA component.

A schematic of the formation of HA on KF is depicted in Fig. 3. The citric ions (*cit*) may bind onto the KF through H bonding, thereby providing binding sites for calcium ions to chelate with the carboxylate from the citric ions, forming a Ca-*cit* complex (Rhee and Tanaka 2000; Cawthray *et al.* 2015). The 3D Ca-*cit* complex provides sites for the creation of clusters of critical size by adsorbing calcium and phosphate. These clusters will then act as nuclei for the crystal growth of HA, leading to porous spheroidal or layered structures within seven or fourteen days, respectively.

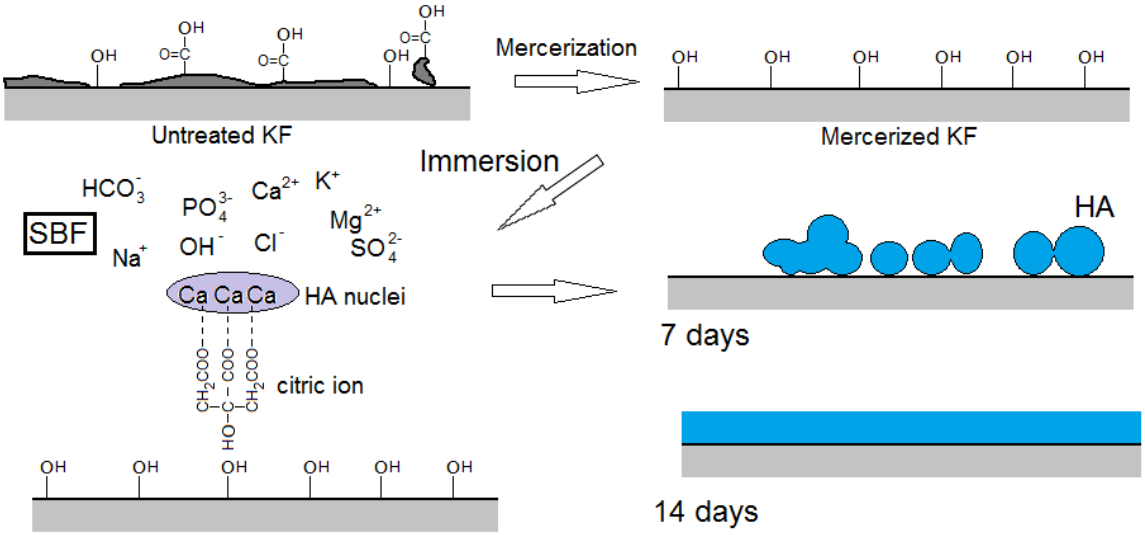

Fig. 3. Schematic illustration for the formation of KF/HA

Tensile Tests

Figure 4 shows the effect of HA deposition on the unit break of KF. Mercerization with NaOH increases the unit break of the KF because of the removal of impurities and the poor crystalline structure of hemicelluloses and lignin. The HA-coated KF seems to retain its mechanical integrity. Only a slight reduction in mechanical integrity was observed. It can be suggested that the deposited HA did not cause any detrimental to the KF and were able to provide stress transfer during the applied loading. An alkaline treatment increases the surface roughness of the KF, resulting in better citric acid adsorption on the fiber surfaces. The grown HA layers can bind onto the KF efficiently using the H bonds, aided by the citric ions and mechanical interlocking between HA and KF. Though the main mechanical load for bone is in compression, this type of material can be suitable to be used at areas where tensional load tend to occur, in areas with a large proportion of cancellous bone.

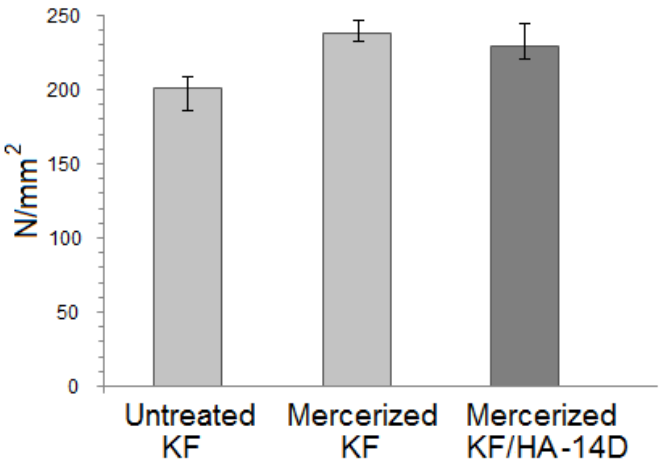

Fig. 4. Unit break of untreated KF, mercerized KF, and mercerized KF soaked in citric acid containing SBF for 14 d.

CONCLUSIONS

1. Biomimetic growth of HA on mercerized KF was successfully demonstrated by adding a chelating agent (citric acid) to form a complex on the interface. The presence of citric acid induced the formation of HA layer on the KF surface after soaking in SBF for fourteen days with a Ca/P ratio of 1.72. FTIR vibrational peaks revealed good interaction between the KF and the HA crystals. Furthermore the crystals were identified to be carbonate-containing HA.
2. Unit break of the KF/HA revealed no significant drop compared to the uncoated KF. Indicating that the mechanical integrity of the KF was intact after modification. The ease with which HA is grown, as well as the economic value of KF, present a high potential for this material to be produced on a large-scale. The main advantage of this newly developed KF/HA is that the deposition substrate can be easily obtained and kept cost effective.

ACKNOWLEDGMENTS

The authors would like to thank Universiti Teknologi Malaysia and the Ministry of Higher Education in Malaysia for providing financial assistance for this research.

REFERENCES CITED

Akil, H., Omar, M. F., Mazuki, A. A. M., Safiee, S., Ishak, Z. A. M., and Bakar, A. A. (2011). "Kenaf fiber reinforced composites: A review," *Materials and Design* 32(8), 4107-4121. DOI:10.1016/j.matdes.2011.04.008

Amini, A. R., Laurencin, C. T., and Nukavarapu, S. P. (2012). "Bone tissue engineering: recent advances and challenges," *Critical Reviews™ in Biomedical Engineering* 40(5), 363-408. DOI:10.1615/CritRevBiomedEng.v40.i5.10

An, J. H., Han, O. S., Kohn, D. H., Park, Y. J., and Song, H. J. (2015). "Characterizations of bone-like apatite powder fabricated using modified simulated body fluid," *Journal of Nanoscience and Nanotechnology* 15(8), 5668-5671. DOI:10.1166/jnn.2015.10467

ASTM D3822. (2007). "Standard test method for tensile properties of single textile fibers," ASTM International, West Conshohocken, PA. DOI: 10.1520/D3822_D3822M-14

Cawthray, J. F., Creagh, A. L., Haynes, C. A., and Orvig, C. (2015). "Ion exchange in hydroxyapatite with lanthanides," *Inorganic Chemistry* 54(4), 1440-1445. DOI: 10.1021/ic502425e

Chen, Q., Baino, F., Pugno, N. M., and Vitale-Brovarone, C. (2013). "Bonding strength of glass-ceramic trabecular-like coatings to ceramic substrates for prosthetic applications," *Materials Science and Engineering: C* 33(3), 1530-1538. DOI: 10.1016/j.msec.2012.12.058

Chen, Q., Baino, F., Spriano, S., Pugno, N. M., and Vitale-Brovarone, C. (2014). "Modelling of the strength–porosity relationship in glass-ceramic foam scaffolds for bone repair," *Journal of the European Ceramic Society* 34(11), 2663-2673. DOI: 10.1016/j.jeurceramsoc.2013.11.041

Costello, L. C., Chellaiah, M., Zou, J., Franklin, R. B., and Reynolds, M. A. (2014). "The status of citrate in the hydroxyapatite/collagen complex of bone; and its role in bone formation," *Journal of Regenerative Medicine and Tissue Engineering* 3, 4. DOI: 10.7243/2050-1218-3-4

Dai, Y., Liu, H., Liu, B., Wang, Z., Li, Y., and Zhou, G. (2015). "Porous β-Ca_2 SiO_4 ceramic scaffolds for bone tissue engineering: In vitro and in vivo characterization," *Ceramics International* 41(4), 5894-5902. DOI: 10.1016/j.ceramint.2015.01.021

Edeerozey, A. M., Akil, H. M., Azhar, A. B., and Ariffin, M. Z. (2007). "Chemical modification of kenaf fibers," *Materials Letters* 61(10), 2023-2025. DOI: 10.1016/j.matlet.2006.08.006

Fernando, A. L., Duarte, M. P., Vatsanidou, A., and Alexopoulou, E. (2015)."Environmental aspects of fiber crops cultivation and use," *Industrial Crops and Products* 68, 105-115. DOI: 10.1016/j.indcrop.2014.10.003

Fiore, V., Di Bella, G., and Valenza, A. (2015). "The effect of alkaline treatment on mechanical properties of kenaf fibers and their epoxy composites," *Composites Part B: Engineering* 68, 14-21.DOI:10.1016/j.compositesb.2014.08.025

Gan, S., Zakaria, S., Chia, C. H., Padzil, F. N. M., and Ng, P. (2015). "Effect of hydrothermal pretreatment on solubility and formation of kenaf cellulose membrane and hydrogel," *Carbohydrate Polymers* 115, 62-68. DOI:10.1016/j.carbpol.2014.08.093

Gao, S., Han, G., Jiang, W., Zhang, Y., and Zhang, X. (2015). "Steam explosion and alkali-oxygen combined effect for degumming of kenaf fiber," *BioResources* 10(3), 5476-5488. DOI:10.15376/biores.10.3.5476-5488

Guo, Y., Lan, J., Zhang, C., Cao, M., Cai, Q., and Yang, X. (2015). "Mineralization on polylactide/gelatin composite nanofibers using simulated body fluid containing amino acid," *Applied Surface Science* 349, 538-548. DOI: 10.1016/j.apsusc.2015.05.047

Huang, C. H., Lai, J. J., Wei, T. Y., Chen, Y. H., Wang, X., Kuan, S. Y., and Huang, J. C. (2015). "Improvement of bio-corrosion resistance for Ti_{42} Zr_{40} Si_{15} Ta_3 metallic glasses in simulated body fluid by annealing within supercooled liquid region," *Materials Science and Engineering: C* 52, 144-150. DOI:10.1016/j.msec.2015.03.056

Juliana, A. H., Paridah, M. T., Rahim, S., Azowa, I. N., and Anwar, U. M. K. (2012). "Properties of particleboard made from kenaf (*Hibiscus cannabinus* L.) as function of particle geometry," *Materials and Design* 34, 406-411. DOI: 10.1016/j.matdes.2011.08.019

Kokubo, T., and Takadama, H. (2006). "How useful is SBF in predicting in vivo bone bioactivity?" *Biomaterials* 27(15), 2907-2915. DOI:10.1016/j.biomaterials.2006.01.017

Kulma, A., Skórkowska-Telichowska, K., Kostyn, K., Szatkowski, M., Skała, J., Drulis-Kawa, Z., and Szopa, J. (2015). "New flax producing bioplastic fibers for medical purposes," *Industrial Crops and Products* 68, 80-89. DOI:10.1016/j.indcrop.2014.09.013

Li, K., Wang, J., Liu, X., Xiong, X., and Liu, H. (2012). "Biomimetic growth of hydroxyapatite on phosphorylated electrospun cellulose nanofibers," *Carbohydrate Polymers* 90(4), 1573-1581. DOI: 10.1016/j.carbpol.2012.07.033

Morimune-Moriya, S., Kondo, S., Sugawara-Narutaki, A., Nishimura, T., Kato, T., and Ohtsuki, C. (2015). "Hydroxyapatite formation on oxidized cellulose nanofibers in a solution mimicking body fluid," *Polymer Journal* 47(2), 158-163. DOI: 10.1038/pj.2014.127

Owen, R., Sherborne, C., Paterson, T., Green, N. H., Reilly, G. C., and Claeyssens, F. (2016). "Emulsion templated scaffolds with tunable mechanical properties for bone tissue engineering," *Journal of the Mechanical Behavior of Biomedical Materials* 54, 159-172. DOI: 10.1016/j.jmbbm.2015.09.019

Pylypchuk, I. V., Petranovskaya, A. L., Gorbyk, P. P., Korduban, A. M., Markovsky, P. E., and Ivasishin, O. M. (2015). "Biomimetic hydroxyapatite growth on functionalized surfaces of Ti-6Al-4V and Ti-Zr-Nb Alloys," *Nanoscale Research Letters* 10(1), 1-8. DOI: 10.1186/s11671-015-1017-x

Razak, S. I. A., Wahman, W. A. W. A., and Yahya, M. Y. (2013). "Novel epoxy resin composites containing polyaniline coated short kenaf bast fibers and polyaniline nanowires: Mechanical and electrical properties," *Journal of Polymer Engineering* 33(6), 565-577. DOI: 10.1515/polyeng-2012-0152

Rhee, S. H., and Tanaka, J. (2000). "Hydroxyapatite formation on cellulose cloth induced by citric acid," *Journal of Materials Science: Materials in Medicine* 11(7), 449-452. DOI:10.1023/A:1008992009826

Rodríguez, K., Renneckar, S., and Gatenholm, P. (2011). "Biomimetic calcium phosphate crystal mineralization on electrospun cellulose-based scaffolds," *ACS Applied Materials & Interfaces* 3(3), 681-689. DOI: 10.1021/am100972r

Rodríguez, K., Sundberg, J., Gatenholm, P., and Renneckar, S. (2014). "Electrospun nanofibrous cellulose scaffolds with controlled microarchitecture," *Carbohydrate Polymers* 100, 143-149. DOI: 10.1016/j.carbpol.2012.12.037

Saba, N., Jawaid, M., Hakeem, K. R., Paridah, M. T., Khalina, A., and Alothman, O. Y. (2015). "Potential of bioenergy production from industrial kenaf (*Hibiscus cannabinus* L.) based on Malaysian perspective," *Renewable and Sustainable Energy Reviews* 42, 446-459. DOI: 10.1016/j.rser.2014.10.029

Sánchez-Ferrero, A., Mata, Á., Mateos-Timoneda, M. A., Rodríguez-Cabello, J. C., Alonso, M., Planell, J., and Engel, E. (2015). "Development of tailored and self-mineralizing citric acid-crosslinked hydrogels for in situ bone regeneration," *Biomaterials* 68, 42-53. DOI: 10.1016/j.biomaterials.2015.07.062

Sola, A., Bellucci, D., Cannillo, V., and Cattini, A. (2011). "Bioactive glass coatings: A review," *Surface Engineering* 27(8), 560-572. DOI: 10.1179/1743294410Y.0000000008

Sukhorukova, I. V., Sheveyko, A. N., Kiryukhantsev-Korneev, P. V., Levashov, E. A., and Shtansky, D. V. (2015). "In vitro bioactivity study of TiCaPCO (N) and Ag-doped TiCaPCO (N) films in simulated body fluid," *Journal of Biomedical Materials Research Part B: Applied Biomaterials*, (In Press) DOI:10.1002/jbm.b.33534

Tomoaia, G., and Pasca, R. D. (2015). "On the collagen mineralization. A review," *Clujul Medical* 88(1), 15-22. DOI: 10.15386/cjmed-359

Wambua, P., Ivens, J., and Verpoest, I. (2003). "Natural fibres: Can they replace glass in fibre reinforced plastics?" *Composites Science and Technology* 63(9), 1259-1264. OI: 10.1016/S0266-3538(03)00096-4

Wang, Q., Zhou, F., Wang, C., Yuen, M. F., Wang, M., Qian, T., and Yan, J. (2015). "Comparison of tribological and electrochemical properties of TiN, CrN, TiAlN and aC: H coatings in simulated body fluid," *Materials Chemistry and Physics* 158, 74-81. DOI: 10.1016/j.matchemphys.2015.03.039

Won, J. S., Lee, T. S., Kim, H. S., Son, H. G., Hong, T. M., Lee, H. W., and Lee, S. G. (2014). "Preparation and characterization of kenaf/soy protein biocomposites," *Journal of Biobased Materials and Bioenergy* 8(2), 221-229. DOI: 10.1166/jbmb.2014.1425

Zaini, N., and Kamarudin, K. S. N. (2014). "Adsorption of carbon dioxide on monoethanolamine (MEA)–impregnated kenaf core fiber by pressure swing adsorption system (PSA)," *Journal Teknologi* 68(5). DOI: 10.11113/jt.v68.3023

Zollfrank, C., Cromme, P., Rauch, M., Scheel, H., Kostova, M. H., Gutbrod, K., and Van Opdenbosch, D. (2012). "Biotemplating of inorganic functional materials from polysaccharides," *Bioinspired, Biomimetic and Nanobiomaterials* 1(1), 13-25. DOI: 10.1680/bbn.11.00002

Article submitted: September 17, 2015; Peer review completed: December 2, 2015; Revised version received: December 9, 2015; Accepted: December 20, 2015; Published: January 12, 2016.
DOI: 10.15376/biores.11.1.1971-1981